INSTITUTE OF PLASMA PHYSICS

NAGOYA UNIVERSITY

Collisional Relaxation of Electron Tail Distribution

Mitsuru YAMAGIWA and Masao OKAMOTO

(Received – Apr. 22, 1985)

IPPJ- 729 May 1985

RESEARCH REPORT

NAGOYA, JAPAN

Collisional Relaxation of Electron Tail Distribution

Mitsuru YAMAGIWA and Masao OKAMOTO

(Received – Apr. 22, 1985)

IPPJ- 729 May 1985

Further communication about this report is to be sent to the Research Information Center, Institute of Plasma Physics, Nagoya University, Nagoya 464, Japan.

Abstract

Relaxation due to the Coulomb collisions of the electron velocity distribution function with a high energy tail is investigated in detail. In the course of the relaxation, a 'saddle' point can be created in velocity space owing to v^{-3} dependence of the deflection rate and a positive slope or a 'dip' appears in the tail direction. The time evolution of the electron tail is studied analytically. A comparison is made with numerical results by using a Fokker-Planck code. Also discussed is the kinetic instability concerned with the positive slope during the relaxation.

§ 1. Introduction

High energy electrons play an important role in confining plasma, for example, in the case of current drive by lower-hybrid waves (LHW) and relativistic electron beams (REB). In lower-hybrid current drive (LHCD), the efficiency increases with the phase velocity of LHW [1] : High energy electrons carrying plasma current should exist in a plasma, though the energetic electron population is much less than the thermal one. Interesting features can be found in such a plasma including wide range of electron velocity, since collisional effect is sensitive to the particle velocity.

Generally the collisional process described by the Fokker-Planck equation is understood by considering the scattering of a test particle in a plasma. The approximate formulas for the slowing down rate (friction coefficient) ν_s^t , and the diffusion coefficients $D_{\parallel}{}^t$ and $D_{\perp}{}^t$ parallel and perpendicular to the velocity of the test particle can be obtained by assuming field particle distributions Maxwellian. [2,3] For velocity range $v \ll v_i, v_e$, where v is the velocity of the test particle, and v_i and v_e are the ion and electron thermal velocities, the slowing down rate and the diffusion coefficients are independent of velocity. Energetic ions with velocity between the ion and electron thermal velocities $v_i \ll v \ll v_e$ slow down mainly by colliding with electrons when v exceeds a critical velocity $v_c = (3\sqrt{\pi} m_e z_i / 4 m_i)^{1/3} v_e$, where m_e, m_i , and z_i are the electron mass, ion mass, and ion charge number, respectively. These ions are produced during neutral beam injection (NBI) or alpha particles due to D-T reactions. If such energetic ions slow down below v_c , the perpendicular diffusion and slowing down by the ion-ion collisions dominate. For high energy elec-

trons (v_i, $v_e \ll v$), which are found, for example, in LHCD, the parallel diffusion is negligibly small. The slowing down rate ν_s^e and the deflection rate which is defined by $\nu_d^e = 2D_{\perp}^e/v^2$ are comparable, $\nu_s^e \sim \nu_d^e (\propto v^{-3})$ and the electron-electron and electron-ion collisions make roughly equal contributions to both processes.

As is seen in these simplified estimations, the relaxation property of high energy electrons (v_i, $v_e \ll v$) is different from that of energetic ions ($v_i \ll v \ll v_e$). The latter is studied, for example, in refs. (4), (5), and (6). Behaviours of runaway electrons (v_i, $v_e \ll v$) in low density Ohmic discharge plasma are also investigated by several authors. [7-14] However, interesting features in the Coulomb collision process for high energy electrons, which will be studied in this work, may be missed owing to dc electric field acceleration.

In this paper, collisional relaxation of the electron distribution with a high energy tail is investigated in detail by studing the Fokker-Planck equation. Such a problem may be worth studying in relation to the 'spectral-gap' between the bulk and LHW-electron resonance region in velocity space during LHCD without dc electric field.

Section 2 is on the analysis of the Fokker-Planck equation, which shows that a 'saddle' point can be created in velocity space and that the time behaviour of the 'saddle' point accompanies a positive slope in the tail direction. In Sec. 3, the tail relaxation is investigated numerically by using a nonlinear Fokker-Planck code [15] and the results are compared with the analysis in Sec. 2. In Sec 4, conclusion and discussion concerned with the kinetic instability originating from the positive slope are presented.

§ 2. Theoretical Analysis

We consider the general properties of the Fokker-Planck collision term. [2,3] The Fokker-Planck equation in the Landau formula is given by

$$\frac{\partial f_a}{\partial t} = \frac{\partial}{\partial \vec{v}} \cdot \sum_b \frac{c_{ab}}{m_a} \int d^3v' \left(\frac{\vec{\vec{I}}}{g} - \frac{\vec{g}\vec{g}}{g^3} \right) \cdot \left[\frac{1}{m_a} \frac{\partial f_a}{\partial \vec{v}} f_b(\vec{v}') - \frac{1}{m_b} \frac{\partial f_b}{\partial \vec{v}'} f_a(\vec{v}) \right] , \tag{1}$$

where $\vec{g}=\vec{v}-\vec{v}'$, $g=|\vec{g}|$, and $c_{ab}=2\pi e_a^2 e_b^2 \ln\Lambda$. In the above equations, e_b, m_b, and f_b are the charge, mass, and distribution function of species-b, respectively, and $\ln\Lambda$ is the Coulomb logarithm.

Suppose f_a has a hole, the minimum extremum, at $\vec{v}=\vec{v}_0$ in velocity space; then $\partial f_a/\partial v_i=0$, $\partial^2 f_a/\partial v_i^2>0$ for each velocity component v_i. We assume that f_b is not negative. Equation (1) at $\vec{v}=\vec{v}_0$ becomes

$$\begin{aligned} \frac{\partial f_a}{\partial t}\Big|_{\vec{v}_0} = & \sum_b \frac{c_{ab}}{m_a} \int d^3v' \frac{\partial}{\partial \vec{v}} \cdot \left(\frac{\vec{\vec{I}}}{g} - \frac{\vec{g}\vec{g}}{g^3} \right) \cdot \left[-\frac{1}{m_b} \frac{\partial f_b}{\partial \vec{v}'} f_a(\vec{v}_0) \right] \\ & + \sum_b \frac{c_{ab}}{m_a} \int d^3v' \left(\frac{\vec{\vec{I}}}{g} - \frac{\vec{g}\vec{g}}{g^3} \right) : \left[\frac{1}{m_a} f_b(\vec{v}') \frac{\partial^2 f_a}{\partial \vec{v} \partial \vec{v}}\Big|_{\vec{v}_0} \right] . \end{aligned} \tag{2}$$

By making use of the relations

$$\frac{\partial}{\partial \vec{v}} \cdot \left(\frac{\vec{\vec{I}}}{g} - \frac{\vec{g}\vec{g}}{g^3} \right) = -\frac{2}{g^3}\vec{g} \tag{3}$$

and

$$\nabla_{v'} \cdot \left(\frac{\vec{g}}{g^3} \right) = -4\pi\delta(\vec{v}'-\vec{v}), \tag{4}$$

the first term of Eq.(2) becomes

$$\frac{8\pi}{m_a} f_a(\vec{v}_0)\left[\sum_b \frac{C_{ab}}{m_b} f_b(\vec{v}_0)\right] > 0 , \tag{5}$$

where it has been assumed that $f_b \to 0$ as $v' \to \infty$. Since

$$\frac{\vec{I}}{g} - \frac{\vec{g}\vec{g}}{g^3} = \frac{\hat{e}_2\hat{e}_2 + \hat{e}_3\hat{e}_3}{g} \tag{6}$$

with $\hat{e}_2$ and $\hat{e}_3$ any two other mutually perpendicular unit vector to $\vec{g}$,

$$\begin{aligned}
&\left(\frac{\vec{I}}{g} - \frac{\vec{g}\vec{g}}{g^3}\right) : \frac{\partial^2 f_a}{\partial \vec{v}\partial \vec{v}}\Big|_{\vec{v}_0} \\
&= \frac{1}{g}\left[\hat{e}_2 \cdot \left(\frac{\partial^2 f_a}{\partial \vec{v}\partial \vec{v}}\right)_{\vec{v}_0} \cdot \hat{e}_2 + \hat{e}_3 \cdot \left(\frac{\partial^2 f_a}{\partial \vec{v}\partial \vec{v}}\right)_{\vec{v}_0} \cdot \hat{e}_3\right] > 0 .
\end{aligned} \tag{7}$$

Thus the second term of Eq.(2) is positive;

$$\sum_b \frac{C_{ab}}{m_a} \int d^3v' \frac{f_b(\vec{v}')}{m_a} \left(\frac{\vec{I}}{g} - \frac{\vec{g}\vec{g}}{g^3}\right) : \frac{\partial^2 f_a}{\partial \vec{v}\partial \vec{v}}\Big|_{\vec{v}_0} > 0 . \tag{8}$$

From the inequalities (5) and (8)

$$\frac{\partial f_a}{\partial t}\Big|_{\vec{v}_0} > 0 . \tag{9}$$

This shows that f_a increases at $\vec{v}=\vec{v}_0$; any hole as an initial perturbation disappears in velocity space. The Fokker-Planck equation does not allow the creation of any hole. When $f_a(\vec{v}_0)=0$, the inequality (9) is also retained. This is the proof of positivity of the distribution function.[2,3] However, in what follows, it will be shown that a 'saddle' point (not a true hole) can be created in velocity space, which leads to a positive slope or a 'dip' in the parallel direction to the magnetic field.

We restrict ourselves to the case when the distribution functions are symmetric about the direction of the magnetic field $\partial f_b/\partial\varphi = 0$, where φ is the azimuthal angle, and write the Fokker-Planck equation in cylindrical coordinates ($v_\parallel, v_\perp$), where $v_\parallel$ is the velocity component parallel to the magnetic field and $v_\perp$ is the normal component. Further we assume $\partial f_a/\partial v_\perp = 0$ at $v_\perp = 0$.

The relaxation of electrons with $v_\perp = 0$ in the parallel velocity space, i.e. on the $v_\parallel$-axis is studied. In the vicinity of $v_\perp = 0$, the Fokker-Planck equation given by Eq.(1) is composed of the terms including $f_e|_{v_\perp=0}$, $\partial^2 f_e/\partial v_\perp^2|_{v_\perp=0}$, $\partial^2 f_e/\partial v_\parallel^2|_{v_\perp=0}$, and $\partial f_e/\partial v_\parallel|_{v_\perp=0}$ for electrons. The $f_e|_{v_\perp=0}$ term is obtained from the l.h.s. of the expression (5). It is complicated but straightforward to obtain the expression for

$$\left(\frac{\delta_{ij}}{g} - \frac{g_i g_j}{g^3}\right)\frac{\partial^2 f_e}{\partial v_i \partial v_j}\Big|_{v_\perp=0} \tag{10}$$

concerned with the $\partial^2 f_e/\partial v_\perp^2|_{v_\perp=0}$ and $\partial^2 f_e/\partial v_\parallel^2|_{v_\perp=0}$ terms in cylindrical coordinates. The gradient of a vector $\partial f_e/\partial \vec{v}$ is given by

$$\frac{\partial^2 f_e}{\partial v_i \partial v_j} = \left(\nabla \frac{\partial f_e}{\partial \vec{v}}\right)_{ij} = \frac{1}{h_i}\frac{(\partial f_e/\partial \vec{v})_j}{\partial \xi_i} + \Gamma^i_{jk}\left(\frac{\partial f_e}{\partial \vec{v}}\right)_k , \tag{11}$$

where $\{\xi_1=v_\perp,\ \xi_2=\varphi,\ \xi_3=v_\parallel\}$ designate the curvilinear coordinates with the scale factors $h_1=h_\perp=1$, $h_2=h_\varphi=v_\perp$, and $h_3=h_\parallel=1$, and Γ^i_{jk} defined by

$$\Gamma^i_{jk} = \frac{1}{h_j h_k}\left(\frac{\partial h_j}{\partial \xi_k}\delta_{ij} - \frac{\partial h_k}{\partial \xi_j}\delta_{ik}\right) \tag{12}$$

is a Christoffel symbol. Taking

$\vec{g} = \{v_\perp - v_\perp' \cos(\varphi-\varphi'),\ v_\perp' \sin(\varphi-\varphi'),\ v_\parallel - v_\parallel'\}$ and $\partial f_e/\partial\varphi = 0$ into

account, we obtain

$$
\begin{aligned}
&\left(\frac{\delta_{ij}}{g}-\frac{g_i g_j}{g^3}\right)\frac{\partial^2 f_e}{\partial v_i \partial v_j} \\
&= \frac{\{v_\perp \cos(\varphi-\varphi')\}^2 + (v_\parallel - v_\parallel')^2}{g^3}\ \frac{1}{v_\perp}\frac{\partial f_e}{\partial v_\perp} \\
&+ \frac{v_\perp - 2v_\perp' \cos(\varphi-\varphi')}{g^3}\ \frac{\partial f_e}{\partial v_\perp} \\
&+ \frac{\{v_\perp' \sin(\varphi-\varphi')\}^2 + (v_\parallel - v_\parallel')^2}{g^3}\ \frac{\partial^2 f_e}{\partial v_\perp^2} \\
&- 2(v_\parallel - v_\parallel')\frac{v_\perp - v_\perp' \cos(\varphi-\varphi')}{g^3}\ \frac{\partial^2 f_e}{\partial v_\perp \partial v_\parallel} \\
&+ \frac{v_\perp^2 - 2v_\perp v_\perp' \cos(\varphi-\varphi') + (v_\perp')^2}{g^3}\ \frac{\partial^2 f_e}{\partial v_\parallel^2} \ . \qquad (13)
\end{aligned}
$$

Therefore, at $v_\perp = 0$

$$
\begin{aligned}
&\left(\frac{\delta_{ij}}{g}-\frac{g_i g_j}{g^3}\right)\frac{\partial^2 f_e}{\partial v_i \partial v_j}\Big|_{v_\perp=0} \\
&= \frac{2(v_\parallel - v_\parallel')^2 + (v_\perp')^2}{\{(v_\parallel - v_\parallel')^2 + (v_\perp')^2\}^{3/2}}\frac{\partial^2 f_e}{\partial v_\perp^2}\Big|_{v_\perp=0} \\
&+ \frac{(v_\perp')^2}{\{(v_\parallel - v_\parallel')^2 + (v_\perp')^2\}^{3/2}}\frac{\partial^2 f_e}{\partial v_\parallel^2}\Big|_{v_\perp=0} \ , \qquad (14)
\end{aligned}
$$

where use has been made of the relation

$$
\lim_{v_\perp \to 0}\ \frac{1}{v_\perp}\frac{\partial f_e}{\partial v_\perp} = \frac{\partial^2 f_e}{\partial v_\perp^2}\Big|_{v_\perp=0} \ . \qquad (15)
$$

The $\partial f_e / \partial v_\parallel |_{v_\perp=0}$ term originates from

$$
\sum_{b=e,i}\frac{c_{eb}}{m_e}\int d^3v'\frac{\partial}{\partial v_i}\left(\frac{\delta_{ij}}{g}-\frac{g_i g_j}{g^3}\right)\frac{1}{m_e}\frac{\partial f_e}{\partial v_j} f_b(v') \qquad (16)
$$

and

$$-\sum_{b=e,i}\frac{c_{eb}}{m_e}\int d^3v'\left(\frac{\delta_{ij}}{g}-\frac{g_i g_j}{g^3}\right)\frac{1}{m_b}\frac{\partial f_b}{\partial v_j}\cdot\frac{\partial f_e}{\partial v_i} \tag{17}$$

of Eq.(1). Integrating by parts in the expression (17) and using Eq.(3), we find that generally like-species collisions (electron-electron collisions) do not contribute to the $\partial f_e/\partial \vec{v}$ term: The $\partial f_e/\partial \vec{v}$ term becomes

$$\begin{aligned}&\frac{2}{m_e}\sum_{b=e,i}c_{eb}\left(\frac{1}{m_b}-\frac{1}{m_e}\right)\int d^3v' f_b(\vec{v}')\frac{\vec{g}\cdot\nabla_v f_e}{g^3}\\ &=\frac{2c_{ei}}{m_e}\left(\frac{1}{m_i}-\frac{1}{m_e}\right)\int d^3v' f_i(\vec{v}')\frac{\vec{g}\cdot\nabla_v f_e}{g^3}\ .\end{aligned} \tag{18}$$

At $v_\perp = 0$, $\partial f_e/\partial v_\parallel|_{v_\perp=0}$ term is given by

$$\frac{2c_{ei}}{m_e}\left(\frac{1}{m_i}-\frac{1}{m_e}\right)\int d^3v' f_i(\vec{v}')\frac{g_\parallel}{g^3}\frac{\partial f_e}{\partial v_\parallel}|_{v_\perp=0}\ . \tag{19}$$

From the expressions (5), (14), and (19), we obtain

$$\begin{aligned}\frac{\partial f_e}{\partial t}|_{v_\perp=0}=&\left[\ 8\pi\sum_{b=e,i}\frac{c_{eb}}{m_e^2}\frac{m_e}{m_b}f_b(v_\parallel'=v_\parallel,v_\perp'=v_\perp=0)\ \right]f_e(v_\parallel,v_\perp=0)\\ &+\left[\sum_{b=e,i}\frac{c_{eb}}{m_e^2}\int d^3v' f_b(\vec{v}')\frac{2(v_\parallel-v_\parallel')^2+(v_\perp')^2}{\{(v_\parallel-v_\parallel')^2+(v_\perp')^2\}^{3/2}}\right]\frac{\partial^2 f_e}{\partial v_\perp^2}|_{v_\perp=0}\\ &+\left[\sum_{b=e,i}\frac{c_{eb}}{m_e^2}\int d^3v' f_b(\vec{v}')\frac{(v_\perp')^2}{\{(v_\parallel-v_\parallel')^2+(v_\perp')^2\}^{3/2}}\right]\frac{\partial^2 f_e}{\partial v_\parallel^2}|_{v_\perp=0}\\ &+\frac{2c_{ei}}{m_e}\left(\frac{1}{m_i}-\frac{1}{m_e}\right)\int d^3v' f_i(\vec{v}')\frac{v_\parallel-v_\parallel'}{\{(v_\parallel-v_\parallel')^2+(v_\perp')^2\}^{3/2}}\frac{\partial f_e}{\partial v_\parallel}|_{v_\perp=0}\ .\end{aligned} \tag{20}$$

Equation (20) retains the general property of the Fokker-Planck collision term: If $\vec{v}_0 = (v_\parallel=v_\parallel^0,\ v_\perp=0)$ is the minimum extremum point of f_e with $\partial^2 f_e/\partial v_\perp^2>0$, $\partial^2 f_e/\partial v_\parallel^2>0$, and $\partial f_e/\partial v_\parallel=0$, then $\partial f_e/\partial t|_{\vec{v}_0}>0$ and any hole

tends to be filled. Consequently there exist no minimum extremum point in velocity space.

Consider a electron distribution function with a long tail in the parallel direction, for example, as shown in Fig. 1. Such a distribution often appears in LHCD. In the figure $u=v_{\parallel}/v_e$ and $w=v_{\perp}/v_e$, and the distribution is taken to be Maxwellian for $u \leqq u_c$. If the distribution function has the maxima at $v_{\perp}=0$ in the perpendicular direction ($\partial^2 f_e/\partial v_{\perp}^2 |_{v_{\perp}=0}<0$) and if the second term in Eq.(20) is sufficiently large, $\partial f_e/\partial t |_{v_{\perp}=0}$ may be negative. Indeed the first term in Eq.(20) is generally small, the coefficient of the second derivative term on $v_{\parallel}$ (the third term) is smaller than that on $v_{\perp}$ (the second term), and for the tail part of the distribution function, $| \partial^2 f_e/\partial v_{\parallel}^2 | \ll | \partial^2 f_e/\partial v_{\perp}^2 |$ and $\partial f_e/\partial v_{\parallel} \sim 0$. Thus for the tail part, time evolution of the distribution function described by Eq.(20) can be dominated by the second term, which has the negative contribution to $\partial f_e/\partial t |_{v_{\perp}=0}$, and a positive slope may be created in the parallel distribution because of the v^{-1} dependence of the perpendicular diffusion coefficient. The slower velocity region in the tail distribution tends to relax faster than the higher region. This leads to the formation of a 'dip' in the parallel velocity space ($\partial^2 f_e/\partial v_{\parallel}^2>0$). Since the hole formation is forbidden as a general property, the sign of the second derivative of f_e with respect to $v_{\perp}$ must be kept negative ($\partial^2 f_e/\partial v_{\perp}^2<0$). Thus Eq.(20) indicates that there is a possibility that a 'saddle' point (not a hole) is created in velocity space during the tail relaxation.

We consider the temporal behaviour of the positive slope formed in the parallel velocity space in the course of time. As will be mentioned later in the section on numerical analysis, if the tail electron popula-

tion is much less than the thermal one, each coefficient in Eq.(20) can be evaluated by assuming f_b Maxwellian with the temperature T_b and the density n_b. Since $v_i \ll v_e$, the following expressions are obtained for $v_\parallel \gg v_e$ and $v_\perp = 0$.

$$8\pi \sum_{b=e,i} \frac{C_{eb}}{m_e^2} \frac{m_e}{m_b} f_b(\vec{v}) \sim 8\pi \frac{C_{ee}}{m_e^2} f_e(\vec{v}) , \tag{21}$$

$$\sum_{b=e,i} \frac{C_{eb}}{m_e^2} \int d^3v' f_b(\vec{v}') \frac{2(v_\parallel - v_\parallel')^2 + (v_\perp')^2}{\{(v_\parallel - v_\parallel')^2 + (v_\perp')^2\}^{3/2}}$$

$$\sim \sum_{b=e,i} \frac{C_{eb} n_b}{m_e^2} \frac{2}{v_\parallel} \{(1 - \frac{v_b^2}{v_\parallel^2}) \Phi(\frac{v_\parallel}{\sqrt{2} v_b}) + \sqrt{\frac{2}{\pi}} \frac{v_b}{v_\parallel} \exp(-\frac{v_\parallel^2}{2v_b^2})\} \tag{22}$$

$$\sim \frac{C_{ee} n_e}{m_e^2} \frac{4}{v_\parallel} , \tag{22}'$$

$$\sum_{b=e,i} \frac{C_{eb}}{m_e^2} \int d^3v' f_b(\vec{v}') \frac{(v_\perp')^2}{\{(v_\parallel - v_\parallel')^2 + (v_\perp')^2\}^{3/2}}$$

$$\sim \sum_{b=e,i} \frac{C_{eb} n_b}{m_e^2} \frac{2}{v_\parallel} \{\frac{v_b^2}{v_\parallel^2} \Phi(\frac{v_\parallel}{\sqrt{2} v_b}) - \sqrt{\frac{2}{\pi}} \frac{v_b}{v_\parallel} \exp(-\frac{v_\parallel^2}{2v_b^2})\} \tag{23}$$

$$\sim \frac{C_{ee} n_e}{m_e^2} \frac{2}{v_\parallel} (\frac{v_e}{v_\parallel})^2 , \tag{23}'$$

and

$$\frac{2C_{ei}}{m_e} (\frac{1}{m_i} - \frac{1}{m_e}) \int d^3v' f_i(\vec{v}') \frac{v_\parallel - v_\parallel'}{\{(v_\parallel - v_\parallel')^2 + (v_\perp')^2\}^{3/2}}$$

$$\sim -\frac{2C_{ei} n_i}{m_e^2 v_\parallel^2} \{\Phi(\frac{v_\parallel}{\sqrt{2} v_i}) - \sqrt{\frac{2}{\pi}} \frac{v_\parallel}{v_i} \exp(-\frac{v_\parallel^2}{2v_i^2})\}$$

$$\sim -\frac{2C_{ei} n_i}{m_e^2 v_\parallel^2} \tag{24}$$

Here, the expressions (22) and (23) denote the diffusion coefficients $D_\perp^v$ and $\frac{1}{2} D_\parallel^v$, respectively, and Φ (x) is the error function. The perpendicu-

lar temperature is taken to be $T_\perp$; $f_e \propto \exp(-m_e v_\perp^2/2T_\perp)$ for $v_\parallel \gg v_e$. By assuming that the third and fourth terms in Eq.(20) can be neglected initially, the temporal behaviour of the electron distribution function for $v_\parallel \gg v_e$ and $v_\perp = 0$ is governed by

$$\frac{\partial f_e}{\partial t}\Big|_{v \gg v_e, v_\perp=0} = \frac{C_{ee}}{m_e^2}\{8\pi f_e(v_\parallel,\ v_\perp=0) - 4n_e\frac{m_e}{T_\perp}\frac{1}{v_\parallel}\}\ f_e(v_\parallel,\ v_\perp=0) \ . \qquad (25)$$

After the normalization by using $\tau = t/\tau_0$, $\tau_0^{-1} = 8\pi e^4 n_e \ln\Lambda / m_e^2 v_e^3$, $\hat{v}_{e\perp}^2 = T_\perp/m_e v_e^2$, $\hat{f}_e = f_e v_e^3/n_e$, and $u = v_\parallel/v_e$, Eq.(25) becomes

$$\frac{\partial \hat{f}_e(u,\tau)}{\partial \tau} = \hat{f}_e(u,\tau)\{2\pi \hat{f}_e(u,\tau) - \frac{1}{u\ \hat{v}_{e\perp}(u,\tau)}\} \ . \qquad (26)$$

The first term is much smaller than the second, unless u is too large. In the constant $\hat{v}_{e\perp}^2$ approximation, the solution for Eq.(26) is

$$\hat{f}_e(u,\tau) = \hat{f}_e(u,0)\exp(-\frac{\tau}{u\ \hat{v}_{e\perp}^2}) \ . \qquad (27)$$

Equation (27) describes the temporal behaviour of the tail. In the time scale and velocity space under consideration, $\partial \hat{f}_e/\partial\tau$ is negative and $\hat{f}_e$ increases with u; a positive slope is produced in the parallel velocity space. On the other hand, the distribution function remains almost Maxwellian near the bulk region. This results in the formation of a 'dip' in the parallel velocity space and hence a 'saddle' point in velocity space.

At the saddle point; $\vec{v} = \vec{v}_s = (v_\parallel = v_\parallel^s, v_\perp = 0)$, $\partial f_e/\partial v_\parallel |_{\vec{v}_s} \sim 0$ and if the form of the distribution function near $\vec{v}_s$ is taken to be

$$f_e(\bar{v}) = f_e(\bar{v}_s)\ \exp\{\frac{m_e(v_\parallel - v_\parallel{}^s)^2}{2T_\parallel}\}\ \exp(-\frac{m_e v_\perp{}^2}{2T_\perp})\ , \tag{28}$$

then Eq.(20) is reduced to

$$\frac{\partial f_e}{\partial t}|_{\bar{v}_s} = \{8\pi\frac{C_{ee}}{m_e{}^2}f_e(\bar{v}_s)\}\ f_e(\bar{v}_s)$$
$$+\ \frac{C_{ee}n_e}{m_e{}^2}\frac{4}{v_\parallel{}^s}(-\frac{m_e}{T_\perp})f_e(\bar{v}_s)$$
$$+\ \frac{C_{ee}n_e}{m_e{}^2}\frac{2}{v_\parallel{}^s}(\frac{v_e}{v_\parallel{}^s})^2\frac{m_e}{T_\parallel}f_e(\bar{v}_s)\ . \tag{29}$$

Since the second term of the r.h.s. is able to have the largest contribution to Eq.(29), the distribution function at the 'saddle' point decreases possessing the negative time derivative; the 'saddle' point does not tend to be filled, though it drops more slowly with increase in $T_\perp$ due to the perpendicular diffusion. Contrary to this, any hole in velocity space tends to be filled by the Coulomb collisions, as previously mentioned.

§ 3. Numerical Analysis

In this section, numerical results by using a nonlinear Fokker-Planck code [15] are compared with the analysis in the previous section. We solve the Fokker-planck equation with the initial distribution function shown in Fig. 1 in order to investigate the relaxation of the tail dustribution numerically. Computation is carried out in spherical polar coordinates (θ,v), where θ is the polar angle and v is the particle speed. The ion distribution is fixed Maxwellian throughout the computation. The boundary condition at the maximum velocity v_{max} is $f(\theta, v_{max})=0$ with v_{max} = 30. The velocity is normalized by the electron thermal velocity of the

bulk plasma. The mesh numbers are 61 in the θ-direction and 76 in the v-direction. Time step is $\Delta\tau = 0.2$ which is normalized by the collision time of the bulk thermal velocity. The distribution function is normalized by n_e/v_e^3.

Figures 2 and 3 show the contours of the distribution function and the parallel distribution functions along the line with $\theta = 0$ and $\theta = \pi$ which corresponds to $v_\perp = 0$, at $\tau = 10$ (a), $\tau = 20$ (b), and $\tau = 30$ (c). In Fig. 3 solid curves are the numerical solutions, broken curves show the analytic solutions given by Eq.(27), and dotted curves indicate the initial distribution function. A 'saddle' point is formed in the two dimensional velocity space near u= u_c and w=0. The point has the minimum and maximum in the parallel and perpendicular directions. As a result, a positive slope or a 'dip' appears in the parallel velocity space. This is because the distribution is almost Maxwellian near the bulk and owing to the v^{-1} dependence of the coefficient of the perpendicular diffusion which drops the value of the distribution function. Also seen is the increase in the perpendicular temperature due to the perpendicular diffusion; $T_\perp \sim 4\ T_e$ at $\tau = 30$ near the 'saddle' point. These pictures are consistent with the analysis in Sec. 2.

We confirm the consistency through the quantitative comparison. In Fig. 3 the analytic solutions for the tail part (Eq.(27)) are shown by broken curves assuming that $\hat{v}_{e\perp}^2$ increases with u^{-1} and $\hat{v}_{e\perp}^2$ (u= u_c) = 4, $\hat{v}_{e\perp}^2$ (u= v_{max}) = 1.5. A fairly good agreement is seen with numerical results; Eq.(27) describes well the temporal relaxation of the tail. The deviation of the analytic solution from the numerical solution is owing mainly to the simplified estimation of the perpendicular temperature $\hat{v}_{e\perp}^2$.

Figure 4 shows the distribution function integrated over $v_\perp$, <F(u)>

at $\tau = 50$. As can be seen in the figure, a positive slope is also formed in $\langle F(u) \rangle$.

We have also done the calculation by using a linear Fokker-Planck code [16] and found that the results appreciably agree with those by the nonlinear code. Therefore the linear Fokker-Planck coefficients can be used to analyze the tail relaxation. This justifies the approximations in Eqs.(22)-(24). Further, it is checked that the H-theorem is satisfied in the nonlinear calculation; for the entropy density

$$s = - \int d^3v f_e \ln f_e \ , \tag{30}$$

$\partial s/\partial t > 0$. Thus the positive slope formation in the parallel distribution is not contrary to the H-theorem.

§ 4. Discussion and Conclusion

We have investigated collisional relaxation of the electron tail distribution by studying the Fokker-Planck equation. An interesting feature has been found in the collisional process of high energy electrons; a 'saddle' point can be created in the two dimensional velocity space in the course of the relaxation. The parallel distribution along the line with $v_\perp = 0$ or integrated over $v_\perp$ can have a positive slope or a dip There is a consistency between the theoretical analysis and the numerical one by using a Fokker-Planck code. The existence of a 'saddle' point or a positive slope is not inconsistent with the H-theorem.

However, such a distribution function with a positive slope is unstable to the plasma wave instability with $\omega = \omega_{pe} k_\parallel / k$. Plasma waves can

be excited via the Cerenkov resonance interaction in velocity region with the positive slope. Therefore, the positive slope may not appear actually because of the inverse Landau damping. The instability originating from the positive slope was analyzed in relation to the tail formation by dc electric field, [17,18] the relaxation of the injected electron beam, [19] and the 'spectral-gap' in LHCD. [16]

In WT-2 experiment on LHCD with applying LHW to the electron tail formed by electron cyclotron resonance heating (ECRH), [20] the discharge was terminated together with abrupt change in the loop voltage, which is like the tail mode instability. [21] The flat tail extended to the higher velocity region due to the longitudinal diffusion by LHW may trigger the instability via the anomalous Doppler effect. Another possible interpretation is as follows: The collisional relaxation of the seed tail formed by ECRH leads to the formation of the positive slope through the mechanism which is studied in the present paper. Subsequently the $\omega=\omega_{pe}k_{\parallel}/k$ mode can be excited via the Cerenkov resonance (inverse Landau damping), even if no anomalous Doppler effect occurs. The excited plasma waves also interact with the electrons in the anomalous Doppler resonance region to increase the perpendicular energy of the electrons. Such electrons could escape from the inherent magnetic surfaces and the confinement would fail. In this way, the plasma waves excited via the Cerenkov resonance may deteriorate the confinement by producing high perpendicular energy electrons.

Acknowledgements

We would like to thank Prof. H. Momota and Dr. M. Azumi for useful discussions. Use has been made of FACOM VP-100 at the Computer Center of the Institute of Plasma Physics in Nagoya University.

References

1) J.G. Cordey: Plasma Phys. and Controlled Fusion 26 (1984) 123.

2) D.C. Montgomery and D.A. Tidman: *Plasma Kinetic Theory* (McGraw-Hill Book Company, New York, 1964).

3) F.L. Hinton: 'Collisional Transport in Plasma' in *Handbook of Plasma Physics*, Eds. M.N. Rosenbluth and R.Z. Sagdeev (North-Holland Publishing Company, Amsterdam New York Oxford, 1983) Vol. I, Chap. 1.5.

4) T.H. Stix: Plasma Phys. 14 (1972) 367.

5) J.A. Rome, D.G. McAlees, J.D. Callen, and R.H. Fowler: Nucl. Fusion 16 (1976) 55.

6) J.D. Gaffey: J. Plasma Phys. 16 (1976) 149.

7) H. Dreicer: Phys. Rev. 115 (1959) 238; ibid. 117 (1960) 329.

8) A.V. Gurevich: Sov. Phys. JETP 12 (1961) 904.

9) M. Kruskal and I.B. Bernstein: 'On the Theory of Runaway Electrons,' Princeton Plasma Physics Laboratory Report Matt-Q-20 (1962).

10) A.N. Lebedev: Sov. Phys. JETP 21 (1965) 931.

11) A.V. Gurevich and Yu.N. Zhivlyuk: Sov. Phys. JETP 22 (1966) 153.

12) R.M. Kulsrud, Y.C. Sun, N.K. Winsor, and H.A. Fallon: Phys. Rev. Lett. 31 (1973) 690.

13) R.H. Cohen: Phys. Fluids 19 (1976) 239.

14) J.C. Wiley, Duk-In Choi, and Wendell Horton: Phys. Fluids 23 (1980) 2193.

15) M.G. McCoy, A.A. Mirin, and J. Killeen: 'FPPAC--A Two-Dimensional Multispecies Nonlinear Fokker-Planck Package,' Lawrence Livermore Laboratory Report UCRL-85666 (1981).

16) M. Yamagiwa, T. Michishita, and M. Okamoto: to be published in J. Phys. Soc. Jpn.

17) B. Coppi, F. Pegoraro, R. Pozzoli, and G. Rewoldt: Nucl. Fusion 16 (1976) 309.

18) L. Muschietti, K. Appert, and J. Vaclavik: Phys. Fluids 25 (1982) 1187.

19) L. Muschietti, K. Appert, and J. Vaclavik: ibid. 24 (1981) 151.

20) S. Kubo et al.: Phys. Rev. Lett. 50 (1983) 1994.

21) V.V. Parail and O.P. Pogutse: Sov. J. Plasma Phys. 2 (1976) 125; Nucl. Fusion 18 (1978) 303.

Figure Captions

Fig. 1 Contour of the electron distribution function with a long tail in the parallel direction.

$$F(u,w) = \frac{1}{(2\pi)^{3/2}}\exp(-\frac{u^2}{2})\exp(-\frac{w^2}{2}) \quad (\equiv F_N(u,w)) \quad for\ u \leqq u_c \ ,$$

$$F(u,w) = \frac{F_N(u_c,w)}{2}(1 + \frac{u_c^2}{u^2}) \quad (\equiv F_{cb}(u,w)) \quad for\ u_c \leqq u \leqq u_b \ ,$$

$$F(u,w) = F_{cb}(u_b,w)\exp(\frac{u_b^2 - u^2}{2}) \quad for\ u_b \leqq u \ .$$

Here, $u = v_\parallel/v_e$, $w = v_\perp/v_e$, $u_c = 3$, $u_b = 28$, and $v_{max} = 30$.

Fig. 2 Contours of the distribution function at $\tau = 10$ (a), $\tau = 20$ (b), and $\tau = 30$ (c).

Fig. 3 Parallel distribution functions F(u,w=0) at $\tau = 10$ (a), $\tau = 20$ (b), and $\tau = 30$ (c). The solid, broken, and dotted curves indicate the numerical solutions, analytic solutions for the tail part (Eq.(27)), and initial distribution function, respectively. They are truncated at the value 2×10^{-3} .

Fig. 4 Parallel distribution function <F(u)> at $\tau = 50$, which is integrated in the perpendicular direction and truncated at the value 4×10^{-2} .

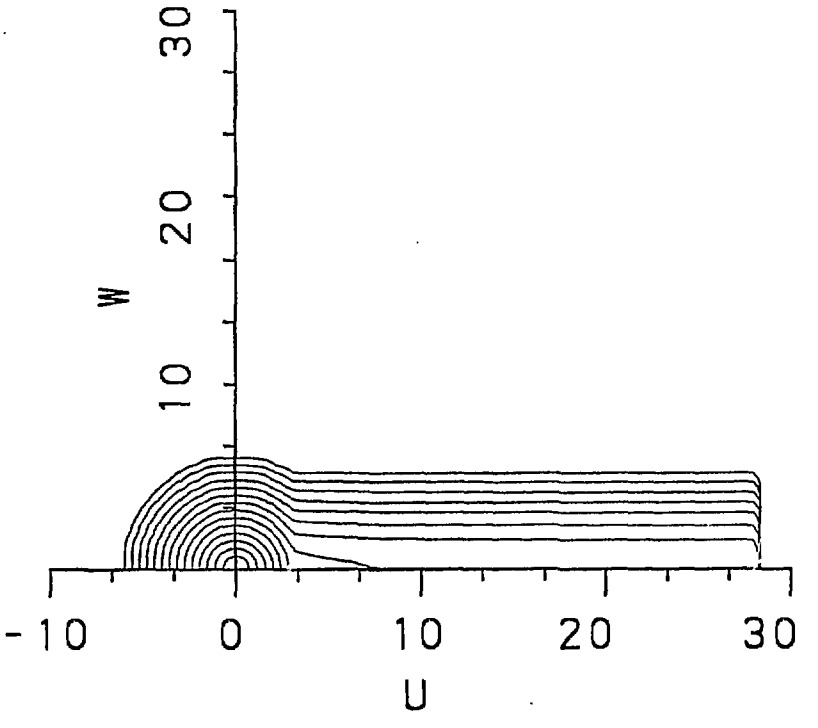

Fig. 1

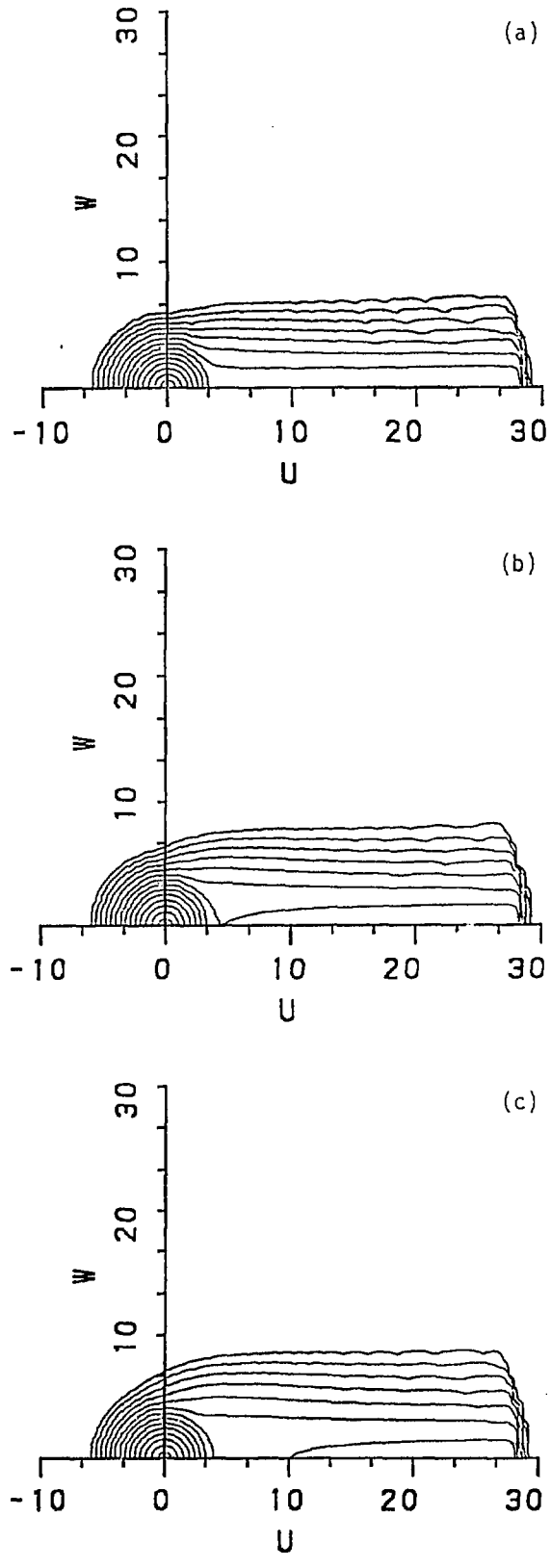
(a)
W
30
20
10
-10
0
10
20
30
U
(b)
W
30
20
10
-10
0
10
20
30
U
(c)
W
30
20
10
-10
0
10
20
30
U

Fig. 2

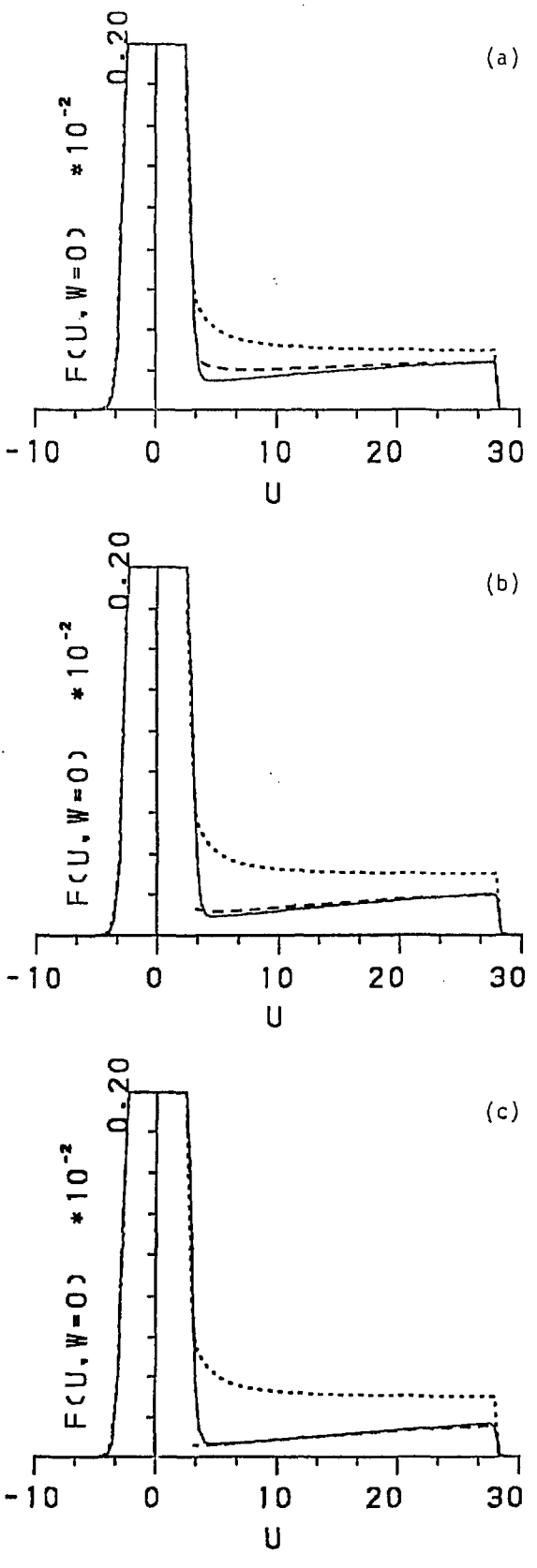
(a)
0.20
F(U, W=0) *10⁻²
-10
0
10
20
30
U
(b)
0.20
F(U, W=0) *10⁻²
-10
0
10
20
30
U
(c)
0.20
F(U, W=0) *10⁻²
-10
0
10
20
30
U

Fig. 3

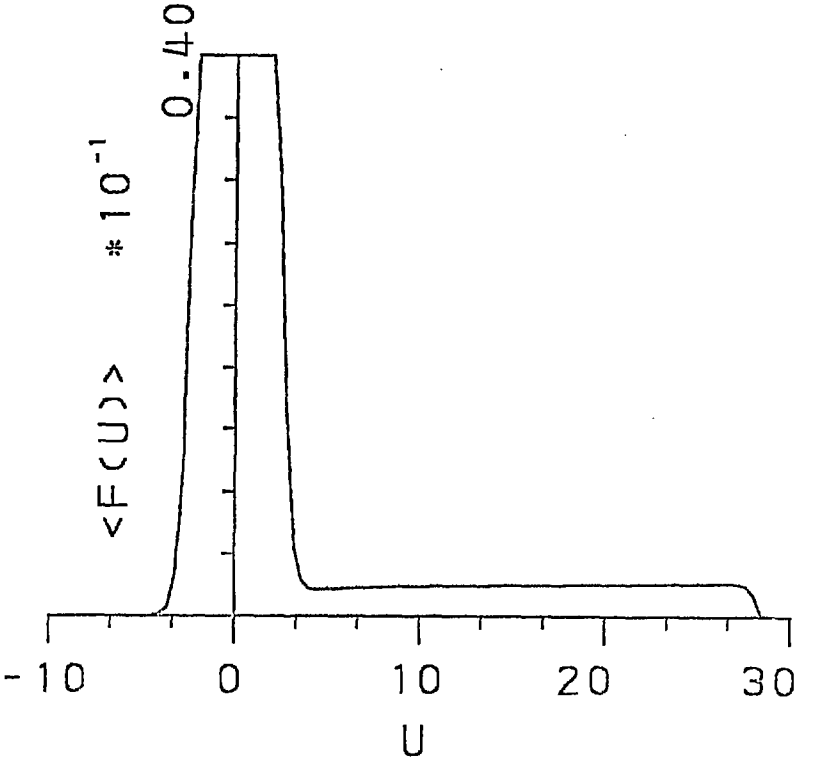

Fig. 4